Clim Dyn (2012) 39:1183–1195
DOI 10.1007/s00382-012-1335-y

Revisiting Asian monsoon formation and change associated with Tibetan Plateau forcing: II. Change

Yimin Liu · Guoxiong Wu · Jieli Hong · Buwen Dong · Anmin Duan · Qing Bao · Linjiong Zhou

Received: 1 August 2011 / Accepted: 7 March 2012 / Published online: 28 March 2012

Abstract Data analysis based on station observations reveals that many meteorological variables averaged over the Tibetan Plateau (TP) are closely correlated, and their trends during the past decades are well correlated with the rainfall trend of the Asian summer monsoon. However, such correlation does not necessarily imply causality. Further diagnosis confirms the existence of a weakening trend in TP thermal forcing, characterized by weakened surface sensible heat flux in spring and summer during the past decades. This weakening trend is associated with decreasing summer precipitation over northern South Asia and North China and increasing precipitation over northwestern China, South China, and Korea. An atmospheric general circulation model, the HadAM3, is employed to elucidate the causality between the weakening TP forcing and the change in the Asian summer monsoon rainfall. Results demonstrate that a weakening in surface sensible heating over the TP results in reduced summer precipitation in the plateau region and a reduction in the associated latent heat release in summer. These changes in turn result in the weakening of the near-surface cyclonic circulation surrounding the plateau and the subtropical anticyclone over the subtropical western North Pacific, similar to the results obtained from the idealized TP experiment in Part I of this study. The southerly that normally dominates East Asia, ranging from the South China Sea to North China, weakens, resulting in a weaker equilibrated Sverdrup balance between positive vorticity generation and latent heat release. Consequently, the convergence of water vapor transport is confined to South China, forming a unique anomaly pattern in monsoon rainfall, the so-called "south wet and north dry." Because the weakening trend in TP thermal forcing is associated with global warming, the present results provide an effective means for assessing projections of regional climate over Asia in the context of global warming.

Keywords Rainfall pattern · Tibetan Plateau thermal forcing · Positive feedback mechanism · Vorticity balance · Global warming

This paper is a contribution to the special issue on Global Monsoon Climate, a product of the Global Monsoon Working Group of the Past Global Changes (PAGES) project, coordinated by Pinxian Wang, Bin Wang, and Thorsten Kiefer.

Y. Liu · G. Wu (✉) · J. Hong · A. Duan · Q. Bao · L. Zhou
State Key Laboratory of Numerical Modeling for Atmospheric Sciences and Geophysical Fluid Dynamics, Institute of Atmospheric Physics, Chinese Academy of Sciences, Beijing, China
e-mail: gxwu@lasg.iap.ac.cn

J. Hong · L. Zhou
Graduate University of Chinese Academy of Sciences, Beijing, China

B. Dong
Department of Meteorology, National Centre for Atmospheric Science, University of Reading, Reading, UK

1 Introduction

Warming of the global surface temperature is unequivocal (IPCC 2007). The IPCC report has shown that the linear warming trend of the surface air temperature is 0.074 °C decade^{-1} for the 100-year period from 1906 to 2005, but it also shows that the rate is almost doubled (0.13 °C decade^{-1}) for the past 50 years, from 1956 to 2005. The warming trend over the Tibetan Plateau (TP) is even more remarkable during this period (Liu and Chen 2000). Based on an analysis of observational data collected from the

China Meteorological Administration (CMA) over the eastern and central TP, Duan et al. (2006a) and Duan and Wu (2008) reported that temporal change in the annual-mean surface atmospheric temperature, T_a, over the plateau increased at a rate of 0.4 °C decade^{-1} during the period of 1980–2003.

Glacier accumulation and melting are sensitive to the surrounding surface temperature, and the accelerated glacial melt over the TP is a direct result of TP warming. In the past half century, 82 % of the plateau's glaciers have retreated; and in the past decade, 10 % of its permafrost has degraded (Qiu 2008). Based on analyses of ice cores from the Dasuopu Glacier (28°23′N, 85°43′E), which is located in the central Himalayas at the southern margin of the TP, Duan et al. (2006b) reported that during the period of 1920–1995 snow accumulation in the Dasuopu ice core decreased by about 500 mm while the temperature in the Northern Hemisphere increased by about 0.5 °C. If this trend continues, it will affect the water supply to hundreds of millions of people in the region.

Beyond local impacts, rapid warming of the TP has far-reaching implications for the climate of the region and even the globe. This is because the TP has a strong impact on the Asian summer monsoon (ASM; e.g., Flohn 1957; Yeh et al. 1957; Wu and Zhang 1998; Ye and Wu 1998; Yanai and Wu 2006). Many studies have suggested that global warming may lead to intensified monsoon rainfall as a result of enhanced land-sea thermal contrast (Meehl and Washington 1993; Meehl 1994; Meehl et al. 1996; Hulme et al. 1998; Anderson et al. 2002; IPCC 2001, 2007). The changes in the TP's thermal status and its thermal contrast with the oceans to its south and east have been used to interpret the interannual variation and change in the ASM (Fu and Fletcher 1985; Zhao and Chen 2001; Hsu and Liu 2003; Wu and Qian 2003; Xu et al. 2006; Zhao et al. 2007), which has shown a distribution of more precipitation in southern India and southern China and less precipitation in northern India and northern China during recent decades. The decreasing trend over Dasuopu, Nepal, northeast India, and Bangladesh was interpreted as a result of the reduced thermal contrast between the TP and the Indian Ocean, as the warming trend over the Indian Ocean during this period was stronger than that over the TP; whereas the increasing trend over South India was considered to be a direct consequence of an increase in evaporated water vapor over the warm Indian Ocean, which provides more water vapor for transport to South India, leading to increased rainfall (Duan et al. 2006b).

Since the end of the 1970s, along with the atmospheric warming over the TP, the East Asian summer monsoon (EASM) has been weakening, which results in a "southern China flood and northern China drought" rainfall pattern, or the so-called "south wet and north dry" (SOWNOD for short; Zhou et al. 2009). To understand the effect of TP warming on climate, Wang et al. (2008, in which three authors of the current study were coauthors) analyzed the variation in surface air temperature averaged over 90 weather stations over the TP. They found a coherent warming trend with an increase of about 1.8 °C over the past 50 years; and this TP warming trend is well correlated with the change in the EASM characterized by the SOWNOD pattern. Based on numerical experiments with the ECHAM4 model, they attempted to reveal the possible link between past temperature changes on the TP and East Asian summer rainfall. Their modeling results suggested that the rising TP temperature could enhance East Asian subtropical frontal rainfall. However, scrutinizing the model results reveals that using TP warming as an index to represent TP thermal forcing and to interpret the TP effect on the EASM might not be appropriate. The specified TP warming in the ECHAM4 model has led to a strengthening of the lower tropospheric subtropical anticyclone over the western North Pacific, associated with an intensified southwesterly monsoon flow to the northwest of the subtropical high, rather than a weakened flow as in the observations (Zhou et al. 2009; Li et al. 2010). In the upper troposphere, the ECHAM4 experiment produced an intensified South Asian high with increased westerlies/easterlies to the north/south of the TP, which is also contrary to the zonal wind change in either ERA-40 or NCEP reanalysis products (Li et al. 2010). The TP warming in the ECHAM4 experiment also generated an enhanced local surface cyclone and precipitation, which is the opposite of the observations, as we will see in our Fig. 2. The discrepancy between observations and the simulation might be model dependent. Thus, it is necessary to test the robustness of the results by using other models to carry out similar experiments. More importantly, increased TP warming does not necessarily indicate increased TP thermal forcing (e.g., Duan and Wu 2008, 2009, and section 3). Since air temperature is one of the atmospheric variables, it may be used for conducting correlation analysis to study the monsoon, but it may not be an appropriate variable for cause-and-effect diagnosis. For this purpose, interpreting the effects of large-scale orographic forcing and the change in thermal forcing on the monsoon becomes critical. Since the formation of the Asian monsoon involves multiscale forcing, including regional forcing of the TP (Liu and Yin 2002; Kitoh 2002, 2004; Abe et al. 2003), and since the TP sensible-heat-driven air-pump (SHAP) in summer leads to the formation of a large-scale cyclonic circulation near the surface that contributes to the intensification of the Asian monsoon (Wu et al. 1997, 2007, 2012), it is more appropriate to link the change in the ASM to the change in TP thermal forcing, especially to the change in surface sensible heat flux over the plateau.

Based on observational data averaged over 71 meteorological stations over the TP for the period of 1980–2003, Duan and Wu (2008) reported a statistically significant reduction in sensible heat transfer from the land surface to the atmosphere, with a diurnal cycle characterized by a weak increasing trend of 1.2 W m^{-2} $decade^{-1}$ at 0000 LST and a much larger declining trend of sensible heat flux from land to air at the rate of −16.3 W m^{-2} $decade^{-1}$ at 1200 LST. Because the maximum sensible heat flux usually occurs at noon and because its trend at 1200 LST shows a marked decline, a significant decreasing trend in the surface sensible heat flux is observed during the period of 1980–2003 over the central and eastern TP. This finding indicates that TP thermal forcing on the ASM system has weakened in recent decades. The present study investigates whether the precipitation trend of the Asian monsoon can be attributed, at least in part, to the weakening in TP thermal forcing.

The remainder of this paper is organized as follows: In Sect. 2, the changes in various meteorological variables and surface sensible heat flux over the TP are investigated based on station observations. The related changes in precipitation and surface pressure over the TP and in the Asian monsoon domain are analyzed in Sect. 3. Section 4 provides a brief description of the atmospheric general circulation model (AGCM) used for this study and the related experiment design. The change in the ASM brought about by increasing or decreasing the amount of surface sensible heating over the TP is diagnosed in Sect. 5. These new results are then compared with observations, and the positive feedback responsible for the development of the ASM is further examined. Finally, the conclusions and discussion are given in Sect. 6.

2 Changes in TP thermal forcing: observations

Wang et al. (2008) employed the PREC/L June–August (JJA) precipitation data and the mean surface air temperature averaged from 90 weather stations over the TP to calculate their correlations. They found that the correlation pattern is similar to the leading rainfall variability pattern over East Asia, presenting both an increase in precipitation in southern China and a decreasing trend in northern China during the 48 years from 1960 to 2007. Here we revisit the topic by using more variables averaged over the TP in JJA and by calculating their correlations with the concurrent precipitation over China. The variables chosen are surface air temperature (T_a), surface ground temperature (T_g), the difference between T_g and T_a (T_g-T_a), wind speed at 10 m above the surface (V), and their product $V\cdot(T_g-T_a)$, which represents a parameter of surface sensible heating defined as PSH. Because the record length for each variable varies from station to station, only those stations with all variable records over the same period are selected for the statistics. As a result, only 24 stations over the TP that satisfy this requirement are selected for the following study.

Figure 1a shows the time evolution of the JJA-mean variables over the TP and their corresponding 5-year running means. All variables exhibit pronounced interannual variation modulated by multidecadal variation. The 5-year running mean surface soil temperature and air temperature both attained a minimum in 1984 and increased rapidly thereafter. The surface air temperature increased from 11.5 °C in 1984 to 12.9 °C in 2007, at a rate of 0.61 °C per decade. This rate is much greater than the previous estimate of 1.8 °C over 50 years (Wang et al. 2008). This difference is caused mainly by the different periods and stations selected for these studies. The surface soil temperature experienced even faster warming, with a rate of 0.74 °C per decade from 1984 to 2007. As a result, the land-air temperature difference (T_g-T_a) also increased after 1980. The evolution of surface wind speed, on the other hand, has a different pattern: the average surface wind speed over the TP increased rapidly from about

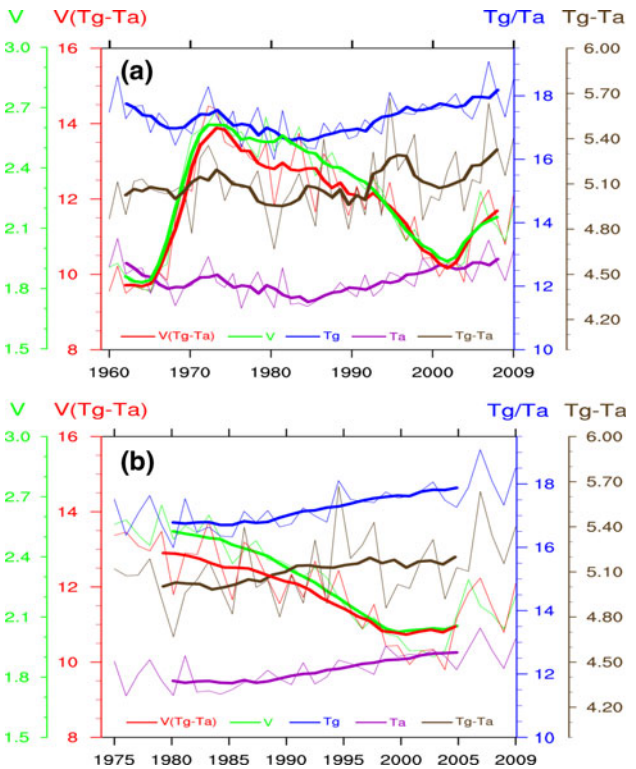

Fig. 1 Annual means of surface soil temperature T_g, surface air temperature T_a, the difference between T_g and T_a, surface wind speed V, and the parameter of surface sensible heat flux $PSH = V\cdot(T_g-T_a)$ averaged over the Tibetan Plateau stations. **a** 1960–2009 and the corresponding 5-year running mean; **b** 1975–2009 and the corresponding 11-year running mean. Units are °C for T_g, T_a, and (T_g-T_a), m s^{-1} for V, and °C m s^{-1} for $PSH = V\cdot(T_g-T_a)$

1.8 m s^{-1} in the mid-1960s to 2.6 m s^{-1} in the early 1970s, then decreased continuously to 1.9 m s^{-1} in 2002, followed by an increasing trend, presenting a 40-year cycle.

The bulk surface sensible heat flux is

$$\text{Surface sensible heat flux} = \rho C_H V \cdot \left(T_g - T_a\right). \quad (1)$$

By considering the impacts of atmospheric stability and thermal roughness from a micro-meteorological perspective, Yang et al. (2009) proposed a new scheme for calculating a time-dependent drag coefficient C_H. Based on station observation data over the TP, Yang et al. (2010) employed the revised Simplified Biosphere Model (SiB2, Sellers et al. 1996) to produce a data set of the atmospheric heat source over the TP and study its climatology and trend. On the other hand, based on a similar data set used by Yang et al. (2010), Zhu (2011) set $C_H = 0.004$, used the monthly climate density ρ to generate another data set of surface sensible heat flux for the TP region, and demonstrated that the spatial and temporal variations in surface sensible heating over the TP calculated from this data set are similar to those from the data set of Yang et al. This is because the relative changes in drag coefficient and density are small compared to those in wind speed and $(T_g - T_a)$ (Yang et al. 2011); the change in surface sensible heating flux (SH) thus depends mainly on the change of $PSH = V \cdot (T_g - T_a)$. Therefore, $PSH = V \cdot (T_g - T_a)$ can be considered a surrogate or parameter of SH as far as climate change is concerned. For this reason, the evolution of $PSH = V \cdot (T_g - T_a)$ is also presented in Fig. 1. Not surprisingly, its pattern closely follows that of V. This is because, according to Fig. 1, the relative change in V is about an order of magnitude larger than the relative change in $(T_g - T_a)$ for the decadal time scale. Therefore,

$$\frac{\Delta SH}{SH} \approx \frac{\Delta V}{V} + \frac{\Delta (T_g - T_a)}{T_g - T_a} \approx \frac{\Delta V}{V}.$$

The result presented in Fig. 1 thus demonstrates that sensible heating over the TP decreased from the early 1970s to the beginning of the twenty first century, in agreement with Duan and Wu (2008) and Yang et al. (2011).

Figure 1a indicates that many meteorological variables are not independent; in fact, they are closely related. As shown in Table 1, the averaged SH parameter PSH is highly correlated with surface wind speed V, and the surface air temperature T_a is highly correlated with the ground surface temperature T_g. It is also interesting to note that the temperature difference $(T_g - T_a)$ is well correlated with both T_g and T_a, and the surface wind speed V is inversely correlated with T_g and T_a; in other words, the stronger the surface wind is, the colder the surface air temperature and surface soil temperature are, and vice versa. Therefore, we must use caution when trying to draw conclusions from correlation analysis.

Table 1 Coefficients of intercorrelation between different meteorological variables and parameters over the Tibetan Plateau

	T_g	T_a	$T_g - T_a$	V	$PSH = V \cdot (T_g - T_a)$
T_g	**1**	**0.95**	**0.62**	**−0.40**	−0.20
T_a		**1**	0.35	−0.45	−0.32
$T_g - T_a$			1	−0.07	0.23
V				1	0.95
$PSH = V \cdot (T_g - T_a)$					1

T_g and T_a denote, respectively, ground surface and air temperature; V, surface wind speed; and PSH, a parameter of surface sensible heat flux. Bold values are above the 95 % significance level

In order to study the climate trends, in the following analysis all the source data used are filtered by an 11-year running mean so that interannual variability and variation due to time scales of less than a decade are filtered out. Figure 1b demonstrates that between 1980 and 2000, the variables T_a, T_g, and $(T_g - T_a)$ possess linear increasing trends, while the uniform decreases in surface wind V and the sensible heating parameter $V \cdot (T_g - T_a)$ are remarkable.

3 Changes in precipitation and surface pressure

Figure 2a and b present the interannual variation in summer precipitation averaged over 60 TP stations from 1961 to 2009 and 74 TP stations from 1975 to 2009, respectively. The red line provides the corresponding linear trend. It demonstrates that after 1960, the mean precipitation averaged over the TP decreased. Figure 2c and d are similar to Fig. 2a and b, respectively, but for surface pressure, which demonstrates an apparent increasing trend between 1980 and 2000 and implies that the summertime surface cyclone system over the TP becomes weaker during this period. The results presented in Fig. 2 correspond well with the decreasing trend in TP surface sensible heating as shown in Fig. 1. Atmospheric thermal adaptation to surface sensible heating will generate a lower-layer cyclonic circulation (Hoskins 1991; Wu and Liu 2000), and a weakening in surface sensible heating will generate a weaker surface cyclone, corresponding to increased surface pressure and decreased rising air and precipitation.

The reanalysis data set of the European Centre for Medium-Range Weather Forecasts, ERA-40, has assimilated surface meteorological observations. By applying Experience Orthogonal Function (EOF) analysis to the summertime (JJA) mean surface pressure over the TP domain (22.9°–41°N, 68.5°–108°E), the leading EOF is obtained and given in Fig. 3. Its variance accounts for 70 % of the total variance for the period of 1960–2002

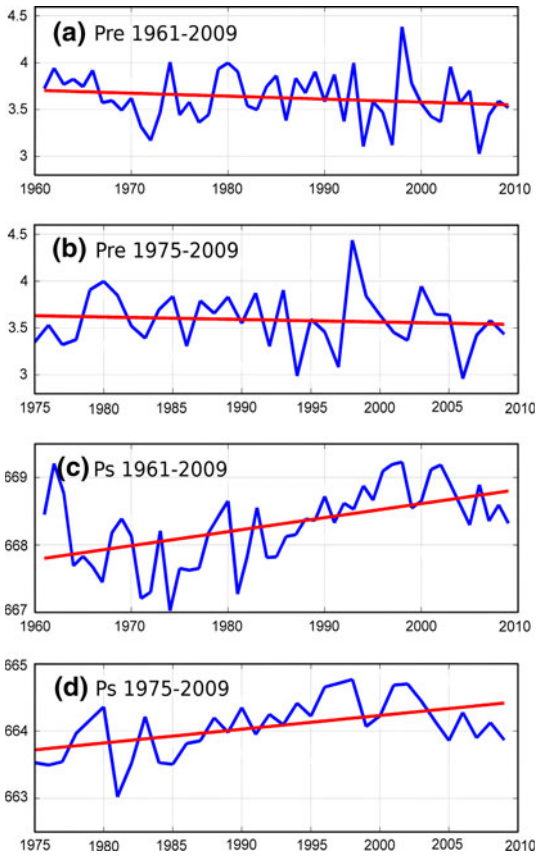

Fig. 2 Annual-mean precipitation (**a**, **b**) and surface pressure (**c**, **d**) averaged over the Tibetan Plateau stations for the period of 1961–2009 (**a**, **c**) and 1975–2009 (**b**, **d**). *Red line* denotes the corresponding trend. Units are mm day^{-1} for precipitation and hPa for surface pressure

(a and b) and 62 % for the period of 1975–2002 (c and d). The spatial distribution of the leading EOF exhibits a region-wide pattern with a maximum on the eastern side of the plateau, while the eigenvector displays a statistically significant increase at the 99 % level, in good agreement with the observations presented in Fig. 2c and d.

Since all the 11-year filtered variables over the TP possess linear trends, the 27-year period of 1980–2006 is selected for the following correlation analysis. Figure 4 shows the correlations of JJA precipitation with different variables averaged over the TP. The relation between precipitation and T_a (Fig. 4a) resembles that in Fig. 1c of Wang et al. (2008). The insignificant difference exists because of different periods selected for the statistics and different numbers of stations included in the TP mean calculations. Since the increasing trend of T_a is almost linear, Fig. 4a thus indicates that after 1980 increasing summer rainfall occurred in northwestern Xinjiang, south of the Yellow River, and the Korean Peninsula, while less precipitation occurred in Pakistan, northeastern India, Bangladesh, and North China. Because T_a is well correlated with T_g and $(T_g - T_a)$ both at the interannual time scale (Table 1) and at time scales longer than a decade (Fig. 1b), the pattern of correlation between precipitation and $T_g/(T_g - T_a)$ is fairly close to that of T_a (figures not shown). On the contrary, the wind speed V and the *PSH* are steadily declining; thus the spatial patterns of their correlations with precipitation resemble those in Fig. 4a but with opposite polarities. Figure 4b shows the pattern of correlation between precipitation and *PSH*. It indicates that decreasing *PSH* over the TP in the last 40 years is associated with an increase in precipitation in South China and a decrease in North China, which is consistent with previous studies (e.g., Xu et al. 2006; Duan and Wu 2008). Is the change in SH over the TP responsible for the observed concurrent changes in precipitation over Asia? If so, what are the physical mechanisms involved? We will address these questions in the next section with sensitivity experiments using an AGCM.

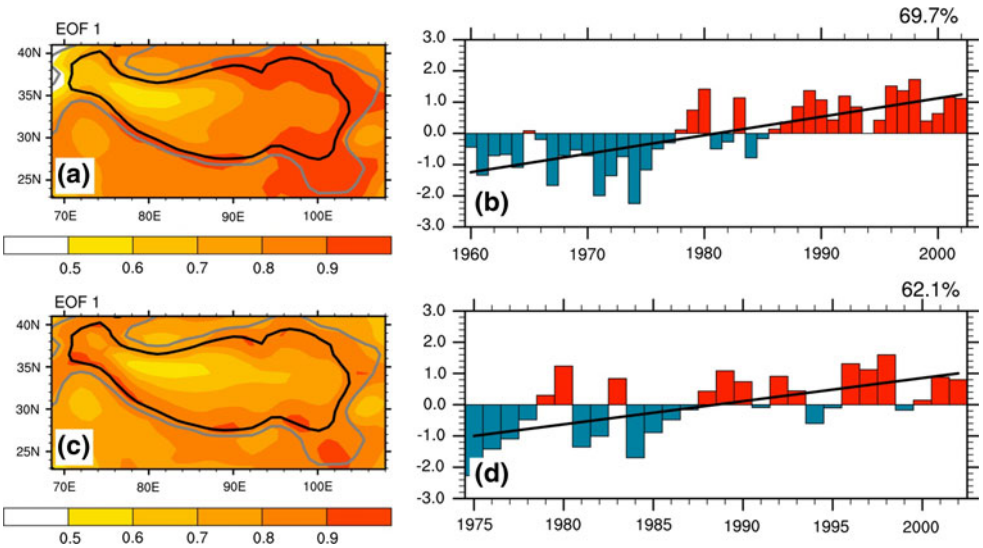

Fig. 3 Leading EOF of the normalized JJA surface pressure over the Tibetan Plateau domain (22.9°–41°N, 68.5°–108°E) during the period of 1960–2002 (**a**, **b**) and 1975–2002 (**c**, **d**) based on the ERA-40 Reanalysis; **a** and **c** are the spatial patterns, and **b** and **d** are the normalized time series. The *straight line* indicates the linear trend, which exceeds the 99 % significance level

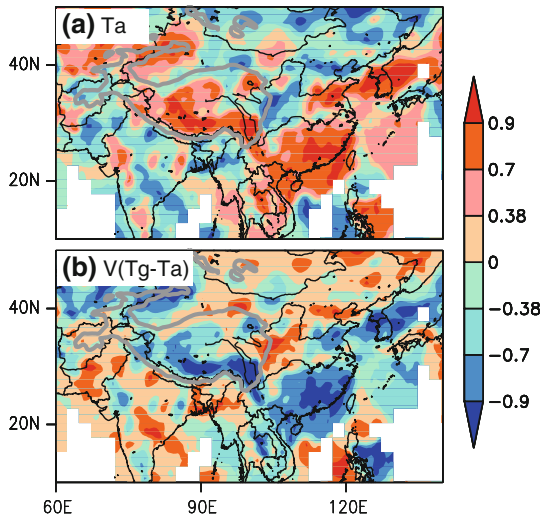

Fig. 4 Distributions of correlation coefficients for the period from 1980 to 2004 and between the JJA precipitation and the TP-averaged **a** T_a and **b** $PSH = V{\cdot}(T_g - T_a)$. The source data have been processed using the 11-year running mean before the correlation calculation was performed

4 AGCM experiment

It should be noted that a good correlation does not always imply causality. The parameters examined in Table 1 and Fig. 4 are all conventional meteorological variables except for *PSH*, which presents the surface sensible heating of the TP. It is important to note that although the TP forcing employed in Part I of this study was introduced by adding the TP into the "Afro-Eurasian continent," the forcing is basically due to its elevated surface sensible heating, as was demonstrated in Liang et al. (2006) and Wu et al. (2007). So the forcing demonstrated by *PSH* is similar to that in Part I. According to the conclusions obtained from the idealized AGCM experiment Exp TPIR in Part I (Wu et al. 2012), a decreasing forcing trend over the TP will result in a weakening of the northern Indian monsoon and East Asian monsoon due to the weakening of the southerly to the southeast of the TP. Thus the distribution of correlation between *PSH* and JJA precipitation presented in Fig. 4b might be considered a cause-and-effect relation. We will next use an AGCM to verify such reasoning and investigate how the reduced surface sensible heating over the TP influences the change in the ASM rainfall.

The AGCM used is the HadAM3, developed at the Hadley Centre of the United Kingdom Met Office. It is a hydrostatic, grid point model that uses an Arakawa B-grid and hybrid vertical coordinates. It is run at a resolution of 2.5° latitude by 3.75° longitude, with 19 vertical levels.

The model uses the radiation scheme developed by Edwards and Slingo (1996) and modified by Cusack et al. (1999), and a prognostic cloud scheme developed by Smith (1990) and modified by Gregory and Morris (1996), which diagnoses cloud ice, cloud water, and cloud cover from the primary model variables of q_T (total moisture) and liquid water potential temperature. The precipitation scheme was developed by Senior and Mitchell (1993), together with the evaporation of precipitation (Gregory 1995). Moist and dry convections are modeled using the mass-flux scheme of Gregory and Rowntree (1990), with the addition of convective downdrafts (Gregory and Allen 1991).

The model includes a land-surface scheme, the met office surface exchange scheme (MOSES), developed by Cox et al. (1999). This scheme includes a representation of the freezing and melting of soil moisture, which leads to more accurate simulation of surface temperature. The model has a formulation of evaporation that includes the dependence of stomatal resistance on temperature, vapor pressure deficit, and CO_2. Each grid box on land is represented by a mixture of five vegetation or plant functional types and four nonvegetated surface types. Surface fluxes and temperatures are calculated separately for each surface type and are aggregated according to the tile fractional coverage before being passed on to the atmospheric model. The standard configuration contains four soil levels at depths of 0.1, 0.25, 0.65, and 2.0 m.

The presence of snow on the ground modifies the land–atmosphere interaction in a number of crucial ways. Snow provides a free source of water for sublimation, and the latent heat associated with melting generally represents a significant portion of the surface energy balance. However, snow also modifies the surface radiative, turbulent, and ground heat fluxes by making the surface brighter and smoother and by insulating the soil from the atmosphere. Each of these effects is represented to some extent within the MOSES. The grid-box mean surface albedo is assumed to vary from its snow-free value, α_0, in the absence of snow, to its deep-snow (temperature-dependent) value of α_{sT} at large snow depth:

$$\alpha = \alpha_0 + (\alpha_{sT} - \alpha_0)\left(1 - e^{\lambda\sigma}\right)$$

where $\lambda = -0.2\ \mathrm{m^2\ kg^{-1}}$, and σ is the snow mass in $\mathrm{kg\ m^{-2}}$. This equation is intended to represent the combined effects of snow depth, heterogeneity, and masking on the surface albedo. The e-folding depth is equivalent to 5 mm of water. The deep-snow albedo has a simple temperature dependence for surface temperature, T_S, above 2 °C:

$$\alpha_{sT} = \alpha_s, \quad \text{for } T_S \leq 2\ ^\circ\mathrm{C}$$

$$\alpha_{sT} = \alpha_s + 0.15\,(\alpha_0 - \alpha_s)(T_S + 2), \quad \text{for } T_S > 2\ ^\circ\mathrm{C}$$

where α_s is the cold deep-snow albedo (0.8) appropriate to the surface. The values of α_0 and α_s are calculated as area-

weighted means of the values specified for each surface type in the grid box (see Table 1 of Cox et al. 1999).

A detailed description of the components of the model can be found in Pope et al. (2000) and references therein. The model has performed well in the atmospheric model intercomparison project (AMIP), producing realistic contemporary patterns of temperature, circulation, and precipitation over Asia (Martin 1999; Martin et al. 2000).

For comparison purposes we followed Wang et al. (2008) in designing our numerical experiments, as summarized in Table 2. Instead of investigating the relation between TP warming and change in the Asian monsoon, we focus on the influence of weakened TP sensible heating on the change in Asian monsoon precipitation and the underlying dynamics. For the control experiment, we use the climatological monthly mean sea surface temperature (SST) and sea ice concentration derived from the HadISST observations (Rayner et al. 2003), and the average concentration of greenhouse gases for the period of 1961–1990. For the two perturbed surface albedo experiments, the bare-land surface albedo, α_0, over the TP in the region of (27.5°N–37.5°N, 75°E–104°E), the same domain as used in Wang et al. (2008), is either decreased or increased by 50 %, hereafter referred to as Exp Albedo-D and Exp Albedo-I, respectively. For each experiment, a 22-year integration starting on December 1 was performed with an initial condition from an earlier integration of the same model forced by the climatological SSTs (Dong et al. 2000). In the following analysis, the results from the first 2 years in each experiment are considered as the model spin-up and are therefore discarded. Thus, the 20-year integrations are used to construct a 20-ensemble mean to reduce uncertainties arising from differing initial conditions. Because the changes in Exps Albedo-I and Albedo-D relative to the control experiment have similar spatial patterns but opposite polarities, the difference between Exps Albedo-I and Albedo-D, which is considered to mimic the recent weakening of the sensible heating source over the TP (Sect. 2; also Duan and Wu 2008), is used to assess the influence of the weakening heating source over the TP on the Asian summer monsoon.

Table 2 List of experiments performed using the AGCM HadAM3

Experiment	Forcing
Control	1961–1990 monthly mean SSTs and sea ice distribution from HadISST. Carbon dioxide, methane, and nitrous oxide are considered to be constant volume concentrations of 332.32, 1.48, and 0.30 ppmv, respectively
Albedo-D	Same as for the control, but bare-land surface albedo over the Tibetan Plateau in the region of (27.5°N–37.5°N, 75°E–104°E) is reduced by 50 %
Albedo-I	Same as for the control, but bare-land surface albedo over the Tibetan Plateau is increased by 50 %

5 Modeled climate change induced by weakened TP forcing

The heat capacity of land is small. In the absence of downward heat penetration under the surface, the net downward radiation energy ($R_n\downarrow$) that reaches and is absorbed by the land surface has to be balanced by the upward sensible heat flux ($SH\uparrow$), latent heat flux ($LH\uparrow$) and outgoing longwave radiation (σT_g^4, where σ is the Stefan–Boltzman constant, and T_g is the surface temperature) from the surface, i.e.,

$$R_n\downarrow \approx SH\uparrow + LH\uparrow + \sigma T_g^4$$

Because the major portion of net downward radiation is solar radiation S, and because the portion of S absorbed by the surface [$=S(1-\alpha)$] decreases with increased albedo α, the immediate response to the increase in surface albedo is a reduction of incoming shortwave solar radiation at the ground surface, resulting in weak local cooling (not shown) and a reduction in the upward surface latent and sensible heat fluxes in the planetary boundary layer throughout the year (Fig. 5a). It also produces a clear seasonal cycle as in the observations, with the largest reduction in sensible heat flux during spring and the largest reduction in latent heat flux during spring and summer. In summer, the upward surface sensible and latent heat fluxes over the TP region decrease by about 11 W m^{-2} (Fig. 5a), with a total decrease of 10–20 W m^{-2} and a local maximum of about 40 W m^{-2} (Fig. 5b). This weakening of the heating source over the TP in the model experiments, which results from an increase in the surface albedo, is similar to the weakening of the surface sensible heating source observed in recent decades (see Fig. 6 in Duan and Wu 2008).

The difference between 30° and 5°N in geopotential thickness between 500 and 200 hPa is one of the indices for presenting the land-sea thermal contrast related to the Asian summer monsoon (Li and Yanai 1996). Because of the reduced heating source of the TP associated with increased surface albedo, stronger negative anomalies of tropospheric temperature presented by the 500–200 hPa geopotential thickness are formed over southern Eurasia relative to the tropical Indian Ocean and the western tropical Pacific (Fig. 5c). These temperature anomalies act to reduce the thermal contrast between the Eurasian continent and adjacent oceans. Therefore, it is anticipated that the anomalies tend to weaken the Asian summer monsoon circulation. The cooling at the surface of the TP stabilizes

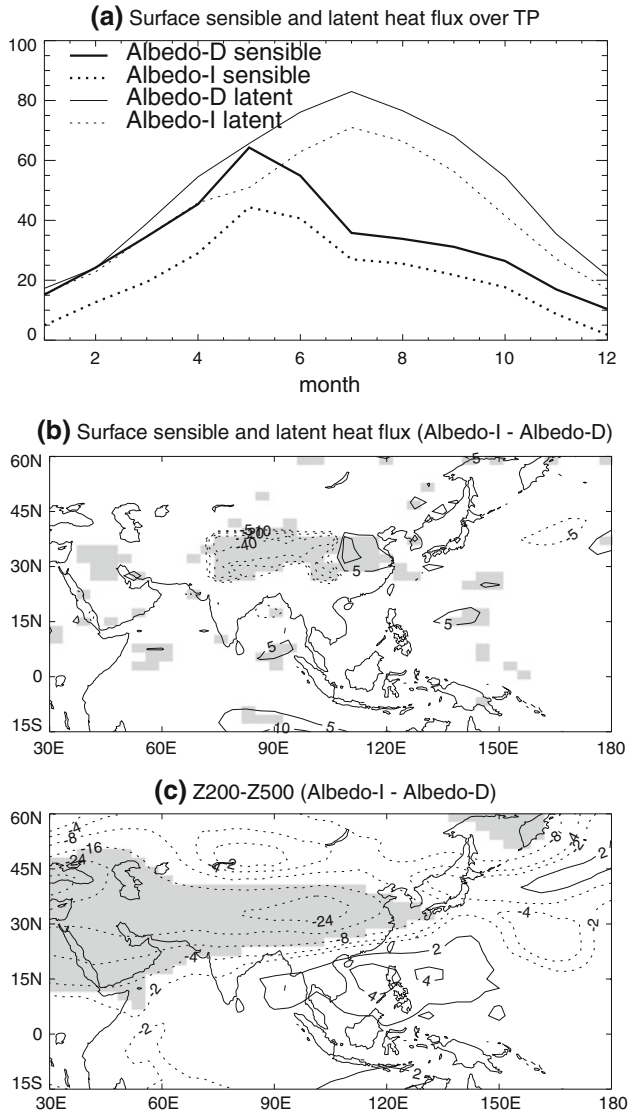

Fig. 5 Monthly evolutions of upward surface sensible and latent heat fluxes (W m^{-2}) over the Tibetan Plateau in the region of (27.5°N–37.5°N, 75°E–104°E) in model experiments (**a**); the difference between Exps Albedo-I and Albedo-D in terms of the JJA-mean surface upward sensible and latent heat flux anomalies (W m^{-2}) (**b**); and geopotential thickness between 200 and 500 hPa (gpm) (**c**). *Shading* indicates regions where anomalies are significant at the 95 % confidence level (*t* test)

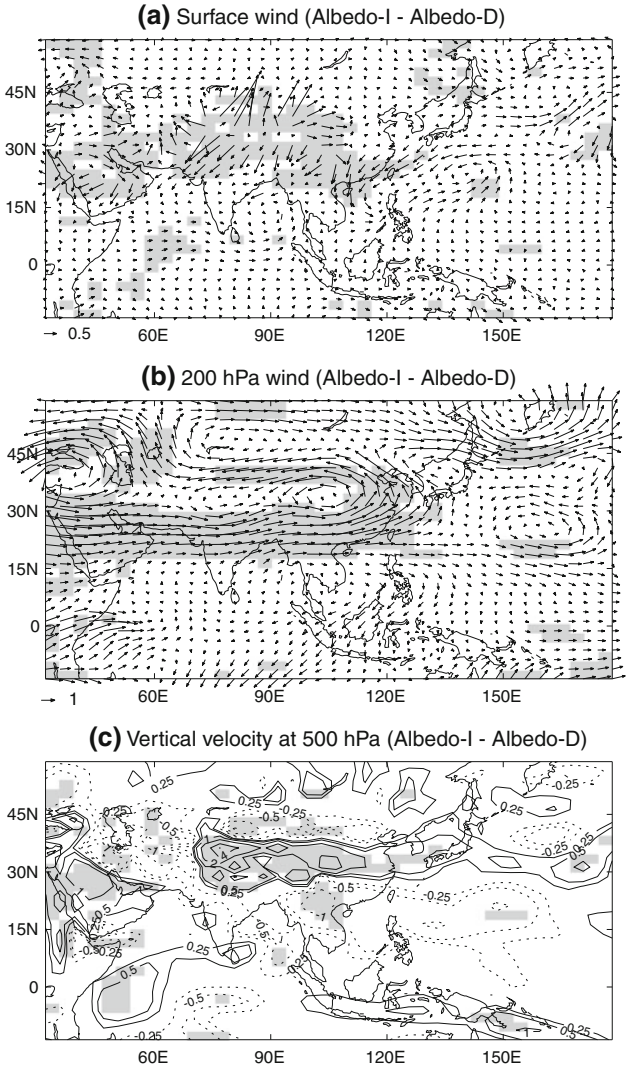

Fig. 6 JJA-mean differences between Exps Albedo-I and Albedo-D in wind (m s^{-1}) and vertical velocity (Pa s^{-1}): **a** surface wind, **b** wind at 200 hPa, and **c** vertical velocity at 500 hPa. *Shading* indicates regions where anomalies are significant at the 95 % confidence level (*t* test)

the atmosphere and leads to weakened convection, resulting in less precipitation locally from spring to autumn (not shown), with a maximum reduction in summer (Fig. 7a). This is in agreement with the observations shown in Fig. 2a and b.

The reduction in sensible heat flux and latent heat release associated with the reduced precipitation in the experiment leads to descent, anomalous anticyclonic circulation and divergence in the lower troposphere, and anomalous cyclonic circulation in the upper layer (Fig. 6). These anomalous circulations provide evidence that surface cooling may intensify the effect of reducing sensible heat flux but cannot outweigh the latter, and this justifies our experiment design for understanding the influence on climate of the weakening trend in TP thermal forcing. This is because the effect of surface cooling on geopotential height decreases with increasing height with a vertically barotropic structure (Thorpe 1985; Hoskins et al. 1985); whereas the effect of a weakened surface sensible heat flux is to generate a vertical baroclinic structure with an anticylonic circulation near the surface and a cyclonic circulation in the upper troposphere (Wu and Liu 2000). The latter is clearly seen from Fig. 6. Furthermore, these anomalous circulations are opposite to the climatological mean circulations (Martin 1999; Martin et al. 2000) and

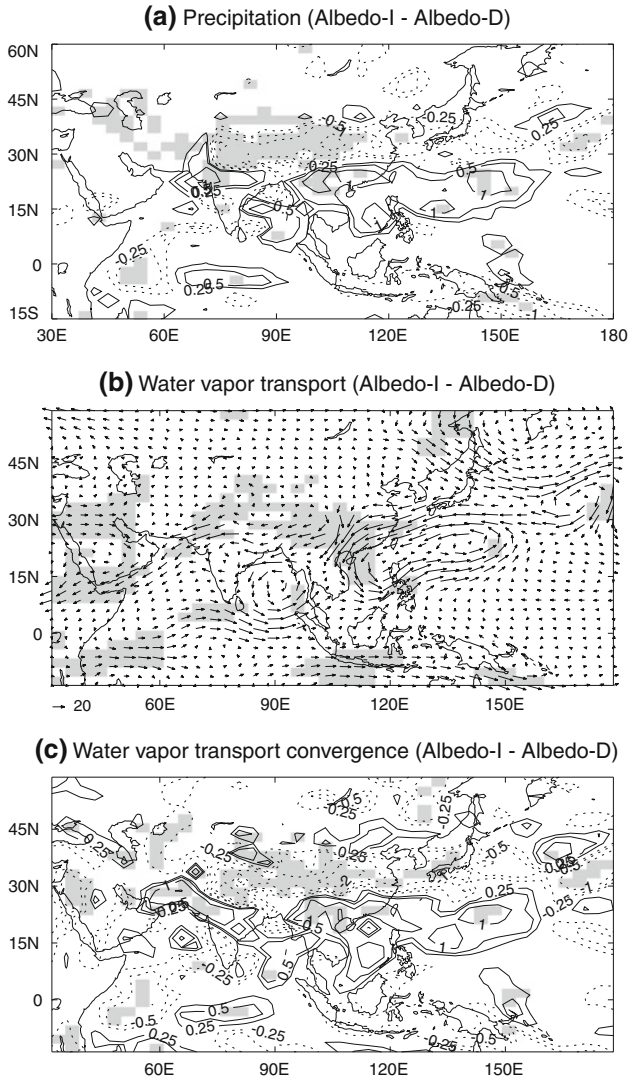

Fig. 7 JJA-mean differences between Exps Albedo-I and Albedo-D: **a** precipitation (mm day^{-1}), **b** vertically integrated water vapor transport (kg m^{-1} s^{-1}), and **c** water vapor transport convergence (kg m^{-2} day^{-1}). *Shading* indicates regions where anomalies are significant at the 95 % confidence level (*t* test)

lead to a weakening of surface wind speed over the TP (not shown), which in return contributes to reduction of the in situ surface sensible and latent heat release. The induced anomalous anticyclonic circulation near the surface in the model experiment also agrees with the observations that show an increasing trend in surface pressure (Fig. 2c, d).

The reduced heating source over the TP induces not only a change in local circulation as highlighted above but also a change in circulation in remote regions (Fig. 6a, b). The change in lower tropospheric circulation over the tropical and subtropical western North Pacific and South China Sea is characterized by a cyclonic circulation anomaly (Fig. 6a) and associated anomalous ascent in the mid-troposphere (Fig. 6c), while an anomalous westerly prevails in the upper troposphere in the subtropics (Fig. 6b). Again, all these changes agree well with the observed changes reported in Zhou et al. (2009) and Li et al. (2010). The anomalous cyclonic circulation in the lower troposphere indicates a weakening of the western Pacific subtropical high and an associated weakening of the EASM circulation. To the west of the anomalous anticyclone over the TP there is a significant moisture convergence over North India (Fig. 7c), thereby indicating a strengthened Indian summer monsoon. Thus, the resultant changes in the weakening of the East Asian monsoon and enhanced Indian monsoon in this experiment agree with the results obtained from the idealized Exp TP as presented in Part I (Fig. 4b in Wu et al. 2012) but have opposite polarities because the imposed TP forcing is weakened in the current experiment but enhanced in the idealized Exp TP, as will be discussed later.

Associated with the weakened EASM circulation is the strongly suppressed precipitation (0.5–2.0 mm day^{-1}) over North China and the increased precipitation over South China (Fig. 7a), corresponding to a change of about 5–10 % relative to the model climatology. This pattern of decreased precipitation in the north and increased precipitation in the south in the experiments is also similar to the observed precipitation trends in China (Fig. 4; also see Fig. 8b in Xu et al. 2006). The increased precipitation over South China extends southward and eastward into the South China Sea, the Philippine Sea, and the western subtropical Pacific, consistent with the local anomalous lower-tropospheric cyclonic circulation (Fig. 6a) and the upper-level anticyclone centered over the southeastern tip of the Indochina Peninsula (Fig. 6b), as well as the mid-tropospheric ascent (Fig. 6c).

Water vapor transport, one of the most important components of the East Asian monsoon system, is strongly associated with the western Pacific subtropical high in the lower troposphere and the East Asia westerly jet stream in the upper troposphere (e.g., Tao and Chen 1987; Zhou and Yu 2005). The anomalous circulations shown in Fig. 6a indicate that the weakened western Pacific subtropical high extends southwestward in response to reduced surface heating over the TP. It is expected that this anomalous circulation pattern results in the enhanced convergence of water vapor transport into the region, as also indicated by the anomalous vertically integrated water vapor transport (Fig. 7b).

The concentration of water vapor in the lower troposphere means that the anomalous total water vapor transport closely resembles the anomalous circulation in the lower troposphere, as shown in Fig. 6a. This anomalous water vapor transport results in anomalous water vapor transport convergence and divergence, as shown in Fig. 7c. The pattern of anomalous water vapor transport

convergence is generally similar to the pattern of anomalous precipitation (Fig. 7a). The convergence of anomalous water vapor transport results in increased precipitation in South China, whereas the divergence of anomalous water vapor transport leads to reduced precipitation in North China. The small magnitude of anomalous water vapor divergence over the TP, relative to the reduction in precipitation, indicates that the reduced evaporation also influences the change in local precipitation in this area. Note that the change in transient moisture flux is not shown in Fig. 7. Based on observation data, Simmonds et al. (1999) and Zhou and Yu (2005) showed that the transient flux plays a negligible role in terms of mean moisture transport and its interannual variability over the monsoon region. The similarity between Fig. 7a and c for many regions indicates that the change in transient moisture flux may play a minor role in this regard.

In these AGCM experiments, the changed elevated forcing is described merely over the TP. It is interesting to compare these results with those from Exp TP in Part I. As shown in Fig. 4b in Part I (Wu et al. 2012), the introduction of TP forcing generates a convergent cyclonic circulation near the surface with a northerly to its west and a southerly to its east. Consequently, the South Asian monsoon precipitation is reduced, whereas the East Asian monsoon is intensified, with more precipitation to the north and less to the south. The weakening in TP sensible heating in the current AGCM experiments induces a divergent anticyclonic circulation near the surface, with a southerly to its west and a northerly to its east (Fig. 6a), resulting in increased southern Asian monsoon rainfall and a weakened East Asian monsoon, with more precipitation confined to the south and less rainfall to the north (Fig. 7a). The results from the sensitive experiments of a complex AGCM thus agree with those from an idealized simple experiment. The underlying mechanism can be viewed from the constraint of potential vorticity conservation at a steady state. Because the weakened TP forcing in spring and summer can generate local anomalous surface anticyclone circulation, the well-organized southerly in the lower troposphere, which normally dominates over East China and the South China Sea during the EASM, becomes weaker. Along this southerly reduction belt, the northward transfer of moisture is reduced, and less rainfall appears over middle and high latitudes. The weakening of the East Asian monsoon there generates less positive potential vorticity; anomalous advection of positive planetary potential vorticity from higher latitudes is then required to keep potential vorticity balanced, and an anomalous northerly thus develops. Consequently, the quasi–steady state achieved through the balance of vorticity generation and advection, which is realized throughout East Asia in the control simulation, is achieved only at lower latitudes in the Albedo-I experiment. This phenomenon makes a large contribution to the occurrence of the "SOWNOD" EASM rainfall anomaly pattern. However, as was discussed in Part I, merely decreasing the TP forcing also results in an increased summer monsoon in northern India. The observed decreasing rainfall over Pakistan, the southern foothills of the TP, and northern India as implied in Fig. 4 should be more closely related to the changed forcing induced by the Iranian Plateau, as was demonstrated by Exp TPIR in Part I.

6 Summary and discussion

Diagnosis based on observational data reveals that many meteorological variables averaged over the TP are closely correlated, and caution must be exercised when pursuing climate variability analysis and making cause-and-effect inferences using one of these variables alone. During the last two decades of the twentieth century, the TP-averaged surface air temperature, surface ground temperature, and their difference have all increased, while the surface wind speed has remarkably decreased. Since for decadal time scales the relative change in wind speed is much greater than the change in temperature difference between the land surface and the air, the surface sensible heating over the TP after the mid-1970s decreased steadily as well. Although the trend in the Asian monsoon rainfall correlates well with the trend of various variables averaged over the TP, it is suggested that only the correlation with the TP surface sensible heating be considered as a cause-and-effect correlation. A weakening trend in TP forcing in spring and summer is correlated with a decreasing JJA precipitation trend over Pakistan, North India, Bangladesh, and North China, and an increasing trend over northwestern China, South China, and Korea as implied in Fig. 4, in agreement with the results of Exp TPIR of Part I as far as the underlying mechanism is concerned.

Numerical experiments based on an AGCM were designed to reveal how the atmosphere responds to the weakening heating source over the TP. The reduction in upward surface sensible heating flux over the TP leads to upper-tropospheric cooling over the Eurasian continent, particularly in tropical and subtropical areas. This cooling results in a reduced thermal contrast between the Eurasian continent and adjacent oceans, thereby weakening the Asian summer monsoon circulation, characterized by the occurrence of an anomalous divergent anticyclonic circulation in the lower troposphere and a cyclonic circulation in the upper troposphere, along with a weakened western Pacific subtropical high. These changes in the lower-tropospheric circulation lead to the convergence of anomalous water vapor transport in North India and South China, and

to the divergence of anomalous water vapor transport in North China, resulting in enhanced precipitation in the northern Indian summer monsoon and increased precipitation in the south and decreased precipitation in the north within the East Asian monsoon region.

The underlying dynamics, as inferred from the combined results of idealized experiments and more realistic climate sensitivity experiments, can be summarized as follows: The reduced sensible heating over the TP in spring and summer acts to weaken the coupling between the lower and upper troposphere, resulting in reduced rainfall in the TP region. The weakening of sensible heating and condensation heating over the TP results in reduced thermal forcing to the atmosphere, and the forced near-surface cyclone is weakened as a result. Consequently, the summertime southerly that usually develops from the South China Sea to central China is weakened, and the coupling between the tropical and subtropical climates is relaxed to some extent. Finally, the equilibrium between positive vorticity generation and latent heat release is weakly developed, resulting in weakening of the EASM. Thus, the monsoon rain belt stays in the south and is unable to move to North China. Therefore, an anomalous pattern is formed, with more rain in the south and less in the north.

It is important to note that the results in this HadAM3 experiment bear a similarity to those from the ECHAM4 experiment in Wang et al. (2008), which indicates both models can reasonably capture monsoon activities. The main difference between these two experiments resides in the experiment design and physical interpretation of the results. In Wang et al. (2008), the TP warming was used as a forcing to explain the changes in the EASM, which produced several inconsistencies with observations, as discussed in Sect. 1. In the present study, the change in surface sensible heating over the TP is used as a forcing to drive the change in the EASM, which produced results that corresponded well with observations. All these again indicate that a good correspondence between the surface air temperature over the TP and precipitation over China does not necessarily mean a good cause-and-effect relation.

Many model results concerning projections of the distribution of anomalous precipitation over China in response to global warming, as reported in the IPCC AR4 (IPCC 2007), show pronounced divergence. Because the change in TP thermal forcing during summer is a consequence of global warming (Duan and Wu 2009), the present insights regarding how changes in TP thermal forcing influence the spatial distribution of EASM rainfall anomalies are significant in terms of obtaining regional climate projections that consider the response to increasing greenhouse gas concentrations in the twenty first century. The current study focused on gaining a process-level understanding by performing sensitivity experiments. This approach can be considered a complementary method of evaluating or assessing regional climate projections based on the outputs of numerical models.

The Asian summer monsoon receives various types of forcing, including not only regional-scale TP forcing, but also continental-scale thermal forcing and local-scale sea-breeze forcing (Liu et al. 2004; Wu et al. 2009). Although temporal changes in regional-scale TP forcing can partially explain the temporal changes in the ASM on a large scale, they cannot explain all of the changes, especially some localized features. In addition, the fact that the TP is warming significantly yet the sensible heat flux is concurrently decreasing is an important observation that is not reflected in this simulation. Ramanathan et al. (2005), Ramanathan and Carmichael (2008) and Lau et al. (2010) proposed that the increasing amount of black carbon and absorbing aerosol due to human activities have strong impacts on the Tg and Ta over the TP. Their results indicate that the long-wave radiation change over the TP is another factor need to be considered when we conduct similar numerical experiments in the future. In any case, further studies are required to reveal the causes of recent regional changes in the ASM, especially in terms of how these changes are related to global climate change.

Acknowledgments This study was jointly supported by the MOST Programme 2010CB950403 and 2012CB417203, CAS program (KZCX2-YW-Q11-01), and NSF of China Projects 40925015, 40875034. BD was supported by the UK National Centre for Atmospheric Science-Climate (NCAS-Climate). Thanks are due to the anonymous reviewers whose suggestions have helped the improvement of the manuscript.

References

Abe M, Kitoh A, Yasunari T (2003) An evolution of the Asian summer monsoon associated with mountain uplift—simulation with the MRI atmosphere-ocean coupled GCM. J Meteorol Soc Jpn 81(5):909–933. doi:10.2151/jmsj.81.909

Anderson DM, Overpeck JT, Gupta AK (2002) Increase in the Asian southwest monsoon during the past four centuries. Science 297(5581):596–599. doi:10.1126/science.1072881

Cox PM, Betts RA, Bunton CB, Essery RLH, Rowntree PR, Smith J (1999) The impact of new land surface physics on the GCM simulation of climate and climate sensitivity. Clim Dyn 15(3):183–203. doi:10.1007/s003820050276

Cusack S, Edward JM, Crowther JM (1999) Investigating k-distribution methods for parameterizing gaseous absorption in the Hadley Centre climate model. J Geophys Res 104(D2):2051–2057. doi:10.1029/1998JD200063

Dong BW, Sutton RT, Jewson SP, Neill AO, Slingo JM (2000) Predictable winter climate in the North Atlantic sector during the 1997–1999 ENSO cycle. Geophys Res Lett 27(7):985–988. doi:10.1029/1999GL010994

Duan A, Wu G (2008) Weakening trend in the atmospheric heat source over the Tibetan Plateau during recent decades. Part I: observations. J Clim 21(13):3149–3164. doi:10.1175/2007JCLI1912.1

Duan A, Wu G (2009) Weakening trend in the atmospheric heat source over the Tibetan Plateau during recent decades. Part II: connection with climate warming. J Clim 22(15):4197–4212. doi:10.1175/2009JCLI2699.1

Duan A, Wu G, Zhang Q, Liu Y (2006a) New proofs of the recent climate warming over the Tibetan Plateau as a result of the increasing greenhouse gases emissions. Chin Sci Bull 51(11):1396–1400. doi:10.1007/s11434-006-1396-6

Duan K, Yao T, Thompson LG (2006b) Response of monsoon precipitation in the Himalayas to global warming. J Geophys Res 111:D19110. doi:10.1029/2006JD007084

Edwards JM, Slingo A (1996) Studies with a flexible new radiation code. I: choosing a configuration for a large-scale model. Q J R Meteor Soc 122(531):689–719. doi:10.1002/qj.49712253107

Flohn H (1957) Large-scale aspects of the "summer monsoon" in South and East Asia. J Meteorol Soc Jpn 75:180–186

Fu C, Fletcher JO (1985) The relationship between Tibet-tropical ocean thermal contrast and interannual variability of Indian monsoon rainfall. J Appl Meteorol 24(8):841–847. doi:10.1175/1520-0450(1985)024<0841:TRBTTO>2.0.CO;2

Gregory D (1995) A consistent treatment of the evaporation of rain and snow for use in large-scale models. Mon Weather Rev 123(9):2716–2732. doi:10.1175/1520-0493(1995)123<2716:ACTOTE>2.0.CO;2

Gregory D, Allen S (1991) The effect of convective scale downdrafts upon NWP and climate simulations. In: Ninth conf on numerical weather prediction, Denver, CO. Am Meteor Soc, pp 122–123

Gregory D, Morris D (1996) The sensitivity of climate simulations to the specification of mixed phase clouds. Clim Dyn 12(9):641–651. doi:10.1007/BF00216271

Gregory D, Rowntree PR (1990) A mass flux convection scheme with representation of cloud ensemble characteristics and stability-dependent closure. Mon Weather Rev 118(7):1483–1506. doi:10.1175/1520-0493(1990)118<1483:AMFCSW>2.0.CO;2

Hoskins BJ (1991) Towards a PV-θ view of the general circulation. Tellus 43(4):27–35. doi:10.1034/j.1600-0870.1991.t01-3-00005.x

Hoskins BJ, McIntyre ME, Robertson AW (1985) On the use and significance of isentropic potential vorticity maps. Q J R Meteorol Soc 111:877–946

Hsu HH, Liu X (2003) Relationship between the Tibetan Plateau heating and East Asian summer monsoon rainfall. Geophys Res Lett 30(20):2066. doi:2010.1029/2003GL017909

Hulme M, Osborn TJ, Johns TC (1998) Precipitation sensitivity to global warming: comparison of observations with HadCM2 simulations. Geophys Res Lett 25(17):3379–3382. doi:10.1029/98GL02562

Intergovernmental Panel on Climate Change (IPCC) (2001) Climate change 2001: the scientific basis—contribution of Working Group I to the Third Assessment Report of the Intergovernmental Panel on Climate Change. Cambridge Univ Press, Cambridge and New York, p 881

Intergovernmental Panel on Climate Change (IPCC) (2007) Climate change 2007: the physical science basis—contribution of Working Group I to the Fourth Assessment Report of the Intergovernmental Panel on Climate Change. Cambridge Univ Press, Cambridge and New York, p 996

Kitoh A (2002) Effect of large-scale mountains on surface climate—a coupled ocean-atmosphere general circulation model study. J Meteorol Soc Jpn 80(5):1165–1181. doi:10.2151/jmsj.80.1165

Kitoh A (2004) Effects of mountain uplift on East Asian summer climate investigated by a coupled atmosphere-ocean GCM. J Clim 17(4):783–802. doi:10.1175/1520-0442(2004)017<0783:EOMUOE>2.0.CO;2

Lau WKM, Kim MK, Kim KM, Lee WS (2010) Enhanced surface warming and accelerated snow melt in the Himalayas and Tibetan Plateau induced by absorbing aerosols. Environ Res Lett 5:025204

Li C, Yanai M (1996) The onset and interannual variability of the Asian summer monsoon in relation to land-sea thermal contrast. J Clim 9:358–375

Li H, Dai A, Zhou T, Lu J (2010) Responses of East Asian summer monsoon to historical SST and atmospheric forcing during 1950–2000. Clim Dyn 34(4):501–514. doi:10.1007/s00382-008-0482-7

Liang XY, Liu YM, Wu GX (2006) Roles of tropical and subtropical land-sea distribution and the Qinghai-Xizang Plateau in the formation of the Asian summer monsoon. Chin J Geophys-Ch 49(4):983–992 (in Chinese)

Liu X, Chen B (2000) Climatic warming in the Tibetan Plateau during recent decades. Int J Climatol 20(14):1729–1742. doi:10.1002/1097-0088(20001130)20:14<1729:AID-JOC556>3.0.CO;2-Y

Liu X, Yin ZY (2002) Sensitivity of East Asian monsoon climate to the uplift of the Tibetan Plateau. Palaeogeogr Palaeocl 183(3–4):223–245. doi:10.1016/S0031-0182(01)00488-6

Liu Y, Wu G, Ren R (2004) Relationship between the subtropical anticyclone and diabatic heating. J Clim 17(4):682–698. doi:10.1175/1520-0442(2004)017<0682:RBTSAA>2.0.CO;2

Martin GM (1999) The simulation of the Asian summer monsoon, and its sensitivity to horizontal resolution, in the UK meteorological office unified model. Q J R Meteor Soc 125(557):1499–1525. doi:10.1002/qj.49712555703

Martin GM, Arpe K, Chauvin F, Ferranti L, Maynard K, Polcher J, Stephenson DB, Tschuck P (2000) Simulation of the Asian summer monsoon in five European general circulation models. Atmos Sci Lett 1(1):37–55. doi:10.1006/asle.2000.0004

Meehl GA (1994) Influence of the land surface in the Asian summer monsoon: external conditions versus internal feedbacks. J Clim 7(7):1033–1049. doi:10.1175/1520-0442(1994)007<1033:IOTLSI>2.0.CO;2

Meehl GA, Washington WM (1993) South Asia summer monsoon variability in a model with doubled atmospheric carbon dioxide concentration. Science 260(5111):1101–1104. doi:10.1126/science.260.5111.1101

Meehl GA, Washington WM, Erickson DJ III, Briegleb BP, Jaumann PJ (1996) Climate change from increased CO_2 and direct and indirect effects of sulfate aerosols. Geophys Res Lett 23(25):3755–3758. doi:10.1029/96GL03478

Pope VD, Gallani ML, Rowntree PR, Stratton RA (2000) The impact of new physical parameterizations in the Hadley Centre climate model: HadAM3. Clim Dyn 16(2–3):123–146. doi:10.1007/s003820050009

Qiu J (2008) China: the third pole. Nature 454(24):393–396. doi:10.1038/454393a

Ramanathan V, Carmichael G (2008) Global and regional climate changes due to black carbon. Nat Geosci 1:221. doi:10.1038/ngeo156

Ramanathan V et al (2005) Atmospheric brown clouds: impacts on South Asian climate and hydrologic cycle. Proc Natl Acad Sci USA 102:5326

Rayner NA, Parker DE, Horton EB, Folland CK, Alexander LV, Rowell DP, Kent EC, Kaplan A (2003) Global analyses of sea surface temperature, sea ice and night marine air temperature since the late nineteenth century. J Geophys Res 108(D14):4407. doi:10.1029/2002JD002670

Sellers P, Randall D, Collatz G, Berry J, Field C, Dazlich D, Zhang C, Collelo G, Bounoua L (1996) A revised land surface parameterization (SiB2) for atmospheric GCMs. Part I: model formulation. J Clim 9(4):676–705

Senior CA, Mitchell JFB (1993) Carbon dioxide and climate: the impact of cloud parameterization. J Clim 6(3):393–418. doi:10.1175/1520-0442(1993)006<0393:CDACTI>2.0.CO;2

Simmonds I, Bi D, Hope P (1999) Atmospheric water vapor flux and its association with rainfall over China in summer. J Clim 12(5):1353–1367. doi:10.1175/1520-0442(1999)012<1353:AWVFAI>2.0.CO;2

Smith RNB (1990) A scheme for predicting layer clouds and their water content in a general circulation model. Q J R Meteor Soc 116(492):435–460. doi:10.1002/qj.49711649210

Tao SY, Chen LX (1987) A review of recent research on the East Asian summer monsoon in China. In: Chang CP, Krishnamurti TN (eds) Review of monsoon meteorology. Oxford University Press, New York, pp 60–92

Thorpe AJ (1985) Diagnosis of balanced vortex structure using potential vorticity. J Atmos Sci 42:97–406

Wang B, Bao Q, Hoskins B, Wu G, Liu Y (2008) Tibetan Plateau warming and precipitation changes in East Asia. Geophys Res Lett 35:L14702. doi:10.1029/2008GL034330

Wu G, Liu Y (2000) Thermal adaptation, overshooting, dispersion, and subtropical anticyclone Part I: thermal adaptation and overshooting. Chin J Atmos Sci 24(4):433–446 (in Chinese)

Wu TW, Qian ZA (2003) The Relation between the Tibetan winter snow and the Asian summer monsoon and rainfall: an observational investigation. J Clim 16(12):2038–2051

Wu G, Zhang Y (1998) Tibetan Plateau forcing and the timing of the monsoon onset over South Asia and the South China Sea. Mon Weather Rev 126(4):913–927. doi:10.1175/1520-0493(1998)126<0913:TPFATT>2.0.CO;2

Wu GX, Li W, Guo H, Liu H, Xue J, Wang Z (1997) Sensible heat driven air-pump over the Tibetan Plateau and its impacts on the Asian summer monsoon. In: Ye DZ (ed) Collections on the memory of Zhao Jiuzhang. Chinese Science Press, Beijing, pp 116–126

Wu G, Liu Y, Wang T, Wan R, Liu X, Li W, Wang Z, Zhang Q, Duan A, Liang X (2007) The influence of the mechanical and thermal forcing of the Tibetan Plateau on the Asian climate. J Hydrometeorol 8(4):770–789. doi:10.1175/JHM609.1

Wu GX, Liu Y, Zhu X, Li W, Ren R, Duan A, Liang X (2009) Multi-scale forcing and the formation of subtropical desert and monsoon. Ann Geophys 27(9):3631–3644. doi:10.5194/angeo-27-3631-2009

Wu G, Liu Y, Liang X, Duan A, Bao Q, Yu J (2012) Revisiting Asian monsoon formation and change associated with Tibetan Plateau forcing—I. Formation. Clim Dyn. doi:10.1007/s00382-012-1334-z

Xu M, Chang CP, Fu C, Qi Y, Robock A, Robinson D, Zhang H (2006) Steady decline of East Asian monsoon winds, 1969–2000: evidence from direct ground measurements of wind speed. J Geophys Res 111:D24111. doi:10.1029/2006JD007337

Yanai M, Wu GX (2006) Effects of the Tibetan Plateau. In: Wang B (ed) The Asian monsoon. Springer, Berlin, pp 513–549. doi:10.1007/3-540-37722-0-13

Yang K, Qin J, Guo X, Zhou D, Ma Y (2009) Method development for estimating sensible heat flux over the Tibetan Plateau from CMA data. J Appl Meteor Climatol 48(12):2474–2486

Yang K, Guo X, He J, Qin J, Koike T (2010) On the climatology and trend of the atmospheric heat source over the Tibetan Plateau: an experiments-supported revisit. J Clim 24:1525–1541

Yang K, Guo XF, Wu BY (2011) Recent trends in surface sensible heat flux on the Tibetan Plateau. Sci China Ser D 54(1):19–28. doi:10.1007/s11430-010-4036-6

Ye DZ, Wu GX (1998) The role of the heat source of the Tibetan Plateau in the general circulation. Meteorol Atmos Phys 67(1–4):181–198. doi:10.1007/BF01277509

Yeh TC, Ye DZ, Lo SW, Chu PC (1957) The wind structure and heat balance in the lower troposphere over the Tibetan Plateau and its surroundings. Acta Meteor Sinica 28:108–121. (in Chinese)

Zhao P, Chen L (2001) Climate features of atmospheric heat source/sink over the Qinghai-Xizang Plateau in 35 years and its relation to rainfall in China. Sci China Ser D 44(9):858–864. doi:10.1007/BF02907098

Zhao P, Zhou Z, Liu J (2007) Variability of Tibetan spring snow and its associations with the hemispheric extratropical circulation and East Asian summer monsoon rainfall: an observational investigation. J Clim 20(15):3942–3955. doi:10.1175/JCLI4205.1

Zhou TJ, Yu RC (2005) Atmospheric water vapor transport associated with typical anomalous summer rainfall patterns in China. J Geophys Res 110(D8):D08104. doi:10.1029/2004JD005413

Zhou T, Gong D, Li J, Li B (2009) Detecting and understanding the multi-decadal variability of the East Asian summer monsoon—recent progress and state of affairs. Meteorol Z 18(4):455–467. doi:10.1127/0941-2948/2009/0396

Zhu XY (2011) Relationship between summertime subtropical multi-scale forcing and the East Asian summer monsoon in interannual and interdecadal variability, Ph. D. thesis, Postgraduate School, Chinese Academy of Science, p 103